*Manuscript
Click here to view linked References

Variable Wind Ripple Migration at Great Sand Dunes National Park, Observed by Timelapse Imagery

Ralph D Lorenz[1] , Andrew Valdez[2]

[1]Applied Physics Laboratory, Johns Hopkins University, Laurel, MD 20723, USA

[2]Great Sand Dunes National Park and Preserve, 11500 Highway 150, Mosca, CO 81146-9798, USA

Submitted 29 Jan, 2011 to Geomorphology

Corresponding Author :

Ralph Lorenz, Applied Physics Laboratory, Johns Hopkins University, Laurel, MD 20723, USA.

Ralph.lorenz@jhuapl.edu tel : +1 443 778 2903 fax : +1 443 778 8939

Abstract

Granule ripples at Great Sand Dunes National Park and Preserve (GSDNPP) were observed with inexpensive digital timelapse cameras over a 70-day period in winter 2010-2011. The ripples migrated during a handful of discrete events - visible ripple movement occurred on only 11 days during the observation period. The movement conditions are documented with hourly and 15-minute records from two nearby weather stations, and by a cup anemometers at the site itself. During the most prominent movement episode when local winds averaged ~10m/s, ripples of several sizes were observed simultaneously and a reciprocal relationship of ripple size and propagation speed was seen, with small (~10cm) ripples moving at ~1.4 cm/min, and larger (~80cm) ripples at ~0.15 cm/min . Ripple sizes and morphologies evolve throughout the observation.

Keywords

Aeolian ripples : bedform dynamics : timelapse camera

1. Introduction

The movement and evolution of Aeolian bedforms, while dramatically fast by geological standards, occur at rates that are inconveniently slow to observe directly. Furthermore, changes are often strongly episodic, driven by environmental conditions such as windspeed, that only occasionally exceed an action threshold. Thus Aeolian process rate measurements demand exceptional patience, and/or luck, from the observer. The approach to measure wind ripple motion has typically (Zimbleman et al., 2009; Yitzaq et al., 2008) been to install markers and to measure motion between visits to a site. Such observations have been important milestones in our understanding of Aeolian processes, but suffer from the fact they record the 'integral' movement over what may be a long period during which motion only occurred for a small fraction. Additionally, particularly in regular ripple patterns, observations can be 'aliased', wherein one cannot be certain that the same feature is being measured.

However, as discussed in Lorenz (2010, 2011) technology developments now mean digital cameras are now available with low enough power consumption and large enough memory capacity to permit automated battery-powered timelapse observation sequences of thousands of images to more comprehensively observe motion and evolution, over anything from hours to months. In particular, in contrast with 'supervised ' field experiments of short duration (e.g. Andreotti et al., 2006) such systems are now sufficiently inexpensive as to be 'expendable' - worth risking in extended unattended observations in the field where damage or theft might occur. In this paper, we describe such a field observation of a set of granule ripples at Great Sand Dunes National Park, over a several-week period. Granule ripples in this area have been studied as analogs of ripple features seen on Mars (Zimbelman et al., 2009).

2. Material and Methods

2.1 Field Site

The study site (figure 1) is a large parabolic dune at 37°41'35.30"N 105°35'11.25"W. The dune is migrating northeast across a sand sheet. This area is within GSDNPPand is 4 km southwest of the main dunefield and is not in an area frequented by visitors. The site is where the dirt road west from the

Great Sand Dunes Oasis general store is blocked by the dune, about 3km from the paved road to the Park. The interior of the dune has many prominent granule ripples.

A barbed wire fence (figure 2) that runs parallel to the road was buried by the arms of the dune, but exposed in the center. Three large wooden fenceposts provided convenient mounting points for our instrumentation.

< FIGURE 1 - Sketchmap >

<FIGURE 2 - site photo >

The ripples generally have crests (figure 3) of granules ~2mm in diameter. Occasionally, if the ground was damp or frozen, the granules tended to collect entirely as discrete structures with granule-free 'interdunes' : more generally finer granules were found between crests. Beneath what was typically a monolayer of granules, finer sand (~200 micron) was found.

< FIGURE 3 - closeup >

Granule ripples commonly form at Great Sand Dunes due to the bimodal sand size distribution present there. Most of the sand is fine grained with a medium sand mode. There is a coarse fraction of very coarse sand, granules and pebbles. At the study site, the course fraction is found in the trough between the arms of the parabolic dune as wind deflation lowers the area and resulting in a lag surface. During strong wind events, the very coarse sand and granules are transported on to the nose of the parabolic dune and organize into granule ripples.

The sand is sourced in the Sangre de Cristo Mountains, which are adjacent to Great Sand Dunes on the east and also the more distal San Juan Mountains which begin 65 km west of Great Sand Dunes. Mineralogical surveys of the dune sand lead to conclusions that the majority of the sand is sourced by volcanic rocks of the San Juan Mountains (Hutchingson, 1968, Wiegand, 1977). The age distribution of zircon in the sand suggests that 70% of the dunefield sand originates in the San Juan Mountains and 30% in the Sangre de Cristos (Madole, 2008). The granules and very coarse sand fraction have a granitic composition. The pebbles are coarse grained metamorphic and ingenious intrusive rocks. The composition and texture of the corse sediment fraction suggest that they are sourced by the nearby Sangre de Cristo Mountains and that streams have flowed in the area.

2.2 Equipment and Setup

We report here on results from two different cameras. First, a modified Brinno Gardenwatchcam ™ (www.brinno.com) was installed on the post (figure 4) on the Eastern arm of the dune, amid the ripples under study. This unit is marketed for horticultural timelapse observations and records images acquired with a 1.3 megapixel CMOS imager to an AVI file on a USB memory stick (the 2 GB stick supplied can hold over 15,000 frames). The unit is nominally powered by 4 alkaline AA cells (which typically have a capacity of ~2000mA-hr), although these do not last long enough to fill the memory stick : we modified the unit to be powered from a separate battery box, in this case using alkaline D-cells (20,000 mA-hr).

< FIGURE 4 - fencepost with camera >

The camera ('1')was set at ~2m height, looking roughly northwards, at an angle of ~20 degrees below horizontal. Based on prior experience with this camera under winter conditions, we set the image acquisition interval to be 10 minutes, which was expected to allow operation for several months. The unit does not record images in darkness, thus after ~60 images at 10 minute spacing in one day, there is a jump to the start of the next day (which is nondeterministic, since it depends on light levels and thus cloud and ground cover). However, the unit records a timestamp on each image.

A second camera (hereafter 'Camera 2') was installed about 30m away on the westernmost fencepost, observing the ripple field in a more or less east-north-eastwards direction (and showing the post with the first camera). This unit was a Wingscapes Plantcam (http://www.wingscapes.com/) which writes individual images (high - 2560x1920, medium - 2048x1536, or low-resolution 640x480 pixels) to a 2GB SD memory card at selectable intervals. This unit, which we used unmodified, has a waterproof casing (like the Gardenwatchcam) which accommodates 4 AA cells. Here we used Lithium AA cells, since these have a higher capacity and tolerate low temperatures better than alkaline battery chemistry. The camera was set to acquire images at 15 minute intervals.

We documented wind conditions at the site with an Inspeed (www.inspeed.com) cup anemometer, installed at the top of the first fencepost. This unit indicates winds with a reed switch closure frequency of 2.5 mph per Hz : we counted these pulses over 5s intervals using a Picaxe 18X datalogger (www.reved.co.uk). The average and peak wind speed, and the casing temperature, was recorded at hourly intervals into the unit's on-board memory (although a coding error, discovered after installation, corrupted the average wind measurement; fortunately, the peak gust measurement was not affected). Finally, Measurement Solutions USB-502 temperature and humidity logger (a unit about the size of a marker pen) was installed next to each camera. A separate cup anemometer, using an electric motor as a transducer, was installed about 15cm above the ground with a Pace Scientific XR-440M datalogger.

During the observation interval, the wire fence was removed. When we retrieved our data on 12 January 2011, we observed the western fenceposts to be loose, having been undermined by sand movement: we re-seated one and removed the other.

3. Results

3.1 Equipment Performance

Camera 1 appears to have operated satisfactorily, recording images up until the night before it was recovered. The video files were examined in a playback application supplied with the camera (which allows stepping through frame-by-frame). An example excerpt from the movie file showing ripple movement on 21-22 November is shown here. In addition to inclusion in the online version of this paper, the video files are available at http://www.lpl.arizona.edu/~rlorenz

< VIDEO >

Some example images are shown in figure 5. Curiously, the video record stops late on 11 January, without images from the morning of recovery. It is possible that the video file was incompletely written, truncating the record (although stopping and starting the camera several times upon recovery, which usually prevents such problems, was performed.) A more plausible scenario is that the camera happened to cease operation that night, which saw very cold temperatures (-20C). Although this was not the first occasion such temperatures were encountered, the probability that the camera will stop when chilled increases with time, as the battery capacity is progressively depleted and thus the voltage droop caused by low temperatures will more likely drop below some threshold.

< FIGURE 5 - Montage of Images >

Camera 2 operated as intended, until the night of November 21, at which point it ceased operation. This was the first night on which temperatures of -10C were encountered during the observation period. Battery voltage droop seems not to be implicated, since the relatively fresh lithium batteries should have been in good condition, even at these temperatures. We speculate that the electronics in this unit - with which we have less experience than the Brinno camera - is less tolerant of low temperatures than are those of camera 1.

One USB temperature logger was found to have stopped during installation, possibly as a result of a reset caused by its battery being knocked out of place. The other USB logger was successfully interrogated, yielding a good temperature and humidity record.

The PICAXE anemometer data logger was interrogated successfully, yielding a case temperature and wind gust history. The XR-440M data appears to have been corrupted; efforts are underway in cooperation with the manufacturer to retrieve these data.

3.2 Ripple Movement and Evolution from Image Data

Visual inspection of the camera 1 record shows ripple migration on only a few days. Using the 80cm spacing of the marker stakes, and the width of the fencepost shadow (the post is 15cm across, but we take into account the distance-dependent broadening (few cm)of the shadow by the 0.5 degree diameter of the sun), the migration distance of ripple features - usually the crest - between image frames can be measured with image analysis tools such as ImageJ. Figure 8 shows the estimated total movement per day over the observation period.

< FIGURE 8 - Ripple Movement over 70 days >

Over the observation period, the morphology, orientation and size of the ripple pattern varies (see figure 5). It was seen that the migration rate varied across the scene, either due to some slope effects on saltation or reputation trajectories directly, variation of the wind field, or sediment supply or all these factors. We will return to these effects shortly in data from Camera 2. Small ripples - often superposed on a larger-scale megaripple pattern - were observed to move more quickly than large ones, as in our previous timelapse experiments (Lorenz, 2011).

Other features of note include the burial of the ripples (and indeed the ground-level cup anemometer) by snow over the period 16-19 December . A tumbleweed is seen to transit the area, and animal prints indicate that the equipment attracted the interest - fortunately without damage to the instrumentation - of a fox or coyote on several occasions. During a ripple migration episode on November 28, several of the marker stakes fell down, presumably as a result of aeolian deflation.

The Camera 2 record is much shorter and of lower spatial resolution than that of Camera 1. However, the image sequence does capture the ripple movement on 21 November. The more distant view (figure 9) sees a larger area of the ripples, and with fewer complicating factors such as foreshortening or the post shadow. We can therefore use a semiautomated analysis procedure to efficiently extract migration rates.

< FIGURE 9 - view from Camera 2 >

First, the images (we use images 578 to 608 of the sequence, spanning 10.03 to 17.33hrs local time - although movement is seen in earlier images that day, images suffer from glare of the rising sun) are contrast-enhanced to make it easier to track features. In our procedure we read each image into the Interactive Data Language (IDL) and subtract a 20-pixel boxcar averaged image from the original (see figure 10) - essentially the same as the ‘unsharp mask’ operator in interactive image analysis tools.

< FIGURE 10- stretched image >

Then, a line from each enhanced image in the sequence is extracted and inserted into a ‘waterfall chart’. Extracted lines from successive images are inserted into progressively lower positions in the chart - thus the horizontal dimension of the chart represents the horizontal dimension of the original scene, while the vertical dimension of the chart corresponds to time. Fixed features in the scene generate vertical lines in the waterfall chart, whereas moving features appear as diagonals, with the slope of the diagonals corresponding to the feature propagation speed across the scene. This ‘waterfall chart’ procedure was introduced in our earlier work (Lorenz, 2011), although the approach here is improved by the better image quality and by the contrast enhancement. We generate 3 separate waterfall charts for the scene (figure 11) , corresponding to different vertical positions in the image, which in turn correspond to different heights on the dune, dominated by different ripple sizes. It is seen that the upper line of the image is dominated by a small-wavelength pattern, which propagates quickly (indeed to the point where more the migration during one camera interval approaches the pattern wavelength, leading to aliasing) whereas progressively lower in the image the pattern wavelength increases and the propagation speed declines.

< FIGURE 11- Waterfall Chart >

3.3 Meteorological Measurements

While the video record is perhaps of interest in its own right, it is of course more useful if the ripple response to the wind can be related to the wind history itself. In their studies of Aeolian ripples at GSDNPP, Zimbleman et al. (2009) use meteorological data from Alamosa airport, 45km away. In fact, more proximate observations exist. Here we use data from two nearby stations. First is the Great Sand Dunes Colorado RAWS (Remote Automatic Weather Station), operated by the National Park Service, data from which was retrieved from the Western Regional Climate Center (http://www.raws.dri.edu/wraws/scaF.html) . The Great Sand Dunes station is at 37° 43' 36" N, 105° 30' 39" , about 10km to the NorthEast of the dune site. Daily summary statistics (average wind, peak gust and many other meteorological variables) are available for download as above (data used here was downloaded 1/12/2011). Hourly data can also be obtained.

The second station within GSDNPP is the Indian Springs Met Station, operated by the US Geological Survey Colorado Water Science Center. This site is at 37°45'50.8" N Longitude 105°37'36.4"W (about 9km to the Northwest of the dune site) and reports only temperature, windspeed and direction, although these data are reported 4 times per hour and are available at http://waterdata.usgs.gov/co/nwis/ (data used in this paper was downloaded 1/12/2011)

It may be noted that the Great Sand Dunes RAWS site (2537m) is topographically more sheltered than Alamosa airport (2297m) or the Indian Springs site (2344m), thus it may be expected to have local slope winds , but may see rather reduced winds driven by regional weather compared with the other sites.

The winds recorded at the site during the movement episode on November 21 seem in broad accord (figure 12) with those measured at Indian Springs, and with the average and gust recorded at the RAWS station. Interestingly, although the RAWS gust that day was larger than that we measured at the ripple site, in general our anemometry record indicates higher wind gusts - by some 50% - at the ripple site than those at the RAWS station (figure 13)

< FIGURE 12 - Nov 21 Winds >

< FIGURE 13 - Correlation Plot >

4. Discussion

4.1 Ripple Migration Rate

We determine migration rates from the waterfall chart (figure 11) by converting the horizontal dimension in pixels to physical length, deriving the scale factor from the camera field of view (52^{o}) and distance (31m); a check against the diameter of the fencepost and other fiducials confirms the scale at ~2.2cm/pixel. Using ImageJ we pick out a number of features A-O (figure 11) and measure their width and spacing, and their propagation speed from the angle across the plot.

Results are shown in figure 14. It is seen that the smallest ripples move most quickly (as would be expected). It is not known with certainty, but seems likely from the imagery and our site inspection, that the smaller ripples have a typically smaller particle size. The propagation speed of ~1.4cm/min approaches the limit at which we could measure speeds without ambiguity due to aliasing (i.e. during the 15-minute interval between images, a ripple moves one wavelength). On the other hand, larger ripples have propagation with uncertainties that formally allow (permitting the slope on the waterfall plot to be bounded by the extent of the ripple) speeds of zero, although with likely values of ~0.15 cm/min. The relationship between ripple size (defined by the width of the bright band in the thresholded image, although we invert the colors in the waterfall chart to improve legibility on the printed page) and propagation speed is a very nearly perfect reciprocal (a best fit in Excel yields an exponent of -1.11 with a correlation coefficient of 0.85). Correlations of speed against ripple spacing, or wavelength (width plus spacing) are poorer.

< FIGURE 14 - migration rates >

Zimbleman et al. (2009, 9 m/s) who observed motion of a 10cm-high granule ripple crest of 10.5cm over 1380 minutes (0.007 cm/min), at a site near the main dunefield of the Great Sand Dunes National Park and Preserve, about 5km away from our site. A 3cm-high ripple was also measured to move 2.1cm in 109 minutes (0.019 cm/min). We estimate the horizontal size of these ripples from their paper to be ~50cm and ~80cm respectively. The overnight measurement of 0.007 cm/min likely underestimates the instantaneous propagation speed, as the windspeed dropped below the probable movement threshold for at least part (~1/4) of this period.

Jerolmack et al. (2006) measure the migration speed of ripples at White Sands National Monument: these ripples were of predominantly gypsum composition. Extrapolating their windspeed vs height measurements (their fig. 4) to our ~2m measurement height gives a freestream windspeed of ~ 10 m/s. The movement of seven ripples (wavelength ~1m, height ~1cm : the width of the ripple may be estimated from their figure 9b to be ~20cm) was measured over 72 minutes, to yield rates of 0.02-0.08 m/hr, or 0.03-0.13 cm/min.

Ripples in fine Sahara sand on the crest of a Egyptian seif dune (Lorenz, 2011) were observed to move at with a windspeed of ~10 m/s (although the friction velocity may have been quite high due to the streamline compression at the crest of the dune.) The wavelength was ~10cm, and the propagation speed (measured by shorter-range timelapse imagery with a higher cadence than in the present work) was determined to be ~3cm/min.

The Zimbelman et al. (2009) and Jerolmack et al. (2006) ripple migration rates are (figure 14) notably smaller than those we have measured. The influence of sediment size or boundary layer properties is difficult to quantify, although it seems that freestream winds during our observation were higher than those during the other work (after all, this was essentially the windiest time over a 70-day period). In any case, the rates we have measured here are lower than those in fine sand on a dune crest, so do not seem unreasonable, even though they exceed those of Jerolmack et al. (2006) and Zimbelman et al. (2009).

4.2 Wind Statistics and Threshold

It is evident from the video record and figure 8 that ripple movement occurs only during a small fraction of time. In part, this is due to winds simply being too weak to cause saltation and reputation, although sometimes moisture (or, indeed, burial by snow !) may suppress movement even if winds are strong enough.

Figure 15 plots the wind gust data over some 7 years from the RAWS station (which may or may not - depending on one's interpretation of figures 12 and 13 - underpredict winds at the site). It is seen that while ~10 m/s winds are considered as a typical threshold (e.g. Zimbelman et al., 2009), such gusts should occur most days at Great Sand Dunes, and indeed gusts of 20 m/s occur some 50% of the time. Further observations covering the summer season are hoped to elucidate the extent to which the contrast between the small number of movements and the large number of days on which winds were strong enough is due to, for example, moisture effects, or instead due to daily gusts being too short-lived to be a good indicator of transport.

As is always the case in Aeolian studies, high-time resolution local wind measurements would be desired, but such aspirations always confront logistical limitations of battery energy, data volume etc. One approach would be to record the mean-cube windspeed over a day, which would more faithfully capture the drift potential than either the peak gust - which might be a very ephemeral windspeed - or the average windspeed (in fact it was an attempt to record such a value that led to the coding error in our PICAXE logger - future efforts will seek to achieve our goal).

4.3 Lessons in Technique

The ease of measurement, and the 'watchability' of the movie, was considerably improved over our initial experiments in Egypt (Lorenz, 2011) by virtue of the mounting on a relatively tall and rigid post. This improved the perspective of the ripple motion, and prevented scene jitter due to camera motion.

An interesting feature in the scene is the moving shadow of the mounting post. This shadow projected on to the variably-sloped scene acts as a useful scalebar. (Additionally, the fact that the shadow's path across the scene varies during the 70-day observation due to the changing solar declination is of interest in educational applications of these data.)

The possibility that the dominant sediment type may evolve during the observation suggests that some means of evaluating this would be useful. One possibility would be a sand trap. Alternatively, some sort of additional instrumentation such as a saltation detector that has a size-dependent response, or a close-up camera able to resolve the size of grains, could be installed.

5. Conclusions

We believe this is the first long-duration (>hrs) continuous field measurement of wind ripple migration. The timelapse imagery approach demonstrated here generates a prodigious amount of data with little effort. Extensive studies beyond the scope of the present paper could be performed, and the data is being archived with the National Park Service to allow other investigators to exploit it. One approach that efficiently condenses certain types of imagery is the ‘waterfall chart’, from which we have extracted a set of ripple migration rates as a function of ripple size, with these variables having an approximately reciprocal relationship. The instantaneous migration rates we have recorded exceed previously-published ripple movement rates, although we note that ripple movement in fact only occurred on about 15% of the days we observed. Further investigation using the methods reported here may help understand the influence of short-term wind variability and moisture on transport in field conditions.

6. Acknowledgements

Camera experiments have been supported in part by the NASA Applied Information Systems Research program. We thank Charlie Bristow for drawing our attention to this excellent site. Phyllis Bovin assisted with the deployment visit, and we thank Fred Bunch for encouragement.

References

Andreotti, B., P. Claudin and O. Pouliquen, Aeolian Sand Ripples: Experimental Study of Fully Developed States, Physical Review Letters, 96, 028001, 2006

Hutchinson, D. M., Provanance of sand in the Great Sand Dunes National Monument, Colorado, PhD dissertation, West Virginia University, 132 pp., 1968

Jerolmack, D. J., D. Mohrig, J. P. Grotzinger, D. A. Fike and W. A. Watters, Spatial grain size sorting in eolian ripples and estimation of wind conditions on planetary surfaces: Application to Meridiani Planum, Mars, Journal of Geophysical Research, 111, E12S02, 2006

Lorenz, R. D., B. Jackson and J. Barnes, Inexpensive Timelapse Digital Cameras for Studying Transient Meteorological Phenomena : Dust Devils and Playa Flooding, Journal of Atmospheric and Oceanic Technology, 27, 246-256, 2010

Lorenz, R. D., Observations of Aeolian Ripple migration on an Egyptian Seif Dune using an Inexpensive Digital Timelapse Camera, Aeolian Research, in press

Madole, R. F., Romig, J. H., Aleinikoff, J. N., VanSistine, D., Yacob, E. Y., On the origin and age of Great Sand Dunes, Colorado, Geomorphology 99, 99-119, 2008

Wiegand, J. P., Dune morphology and sedimentology at Great Sand Dunes National Monument, MS Thesis, Colorado State University, 165 pp., 1977

Yizhaq, H., O. Isenberg, R. Wenkart, H. Tsoar and A. Karnieli, Morphology and dynamics of Aeolian mega-ripples in Nahal Kasuy, southern Israel, Israeli Journal of Earth Science, 57, 149-165, 2009

Zimbelman, J. R., R. P. Irwin III, S. H. Williams, F. Bunch, A. Valdez and S. Stevens, The rate of granule ripple movement on Earth and Mars, Icarus, 203, 71-76, 2009

Figure
Click here to download high resolution image

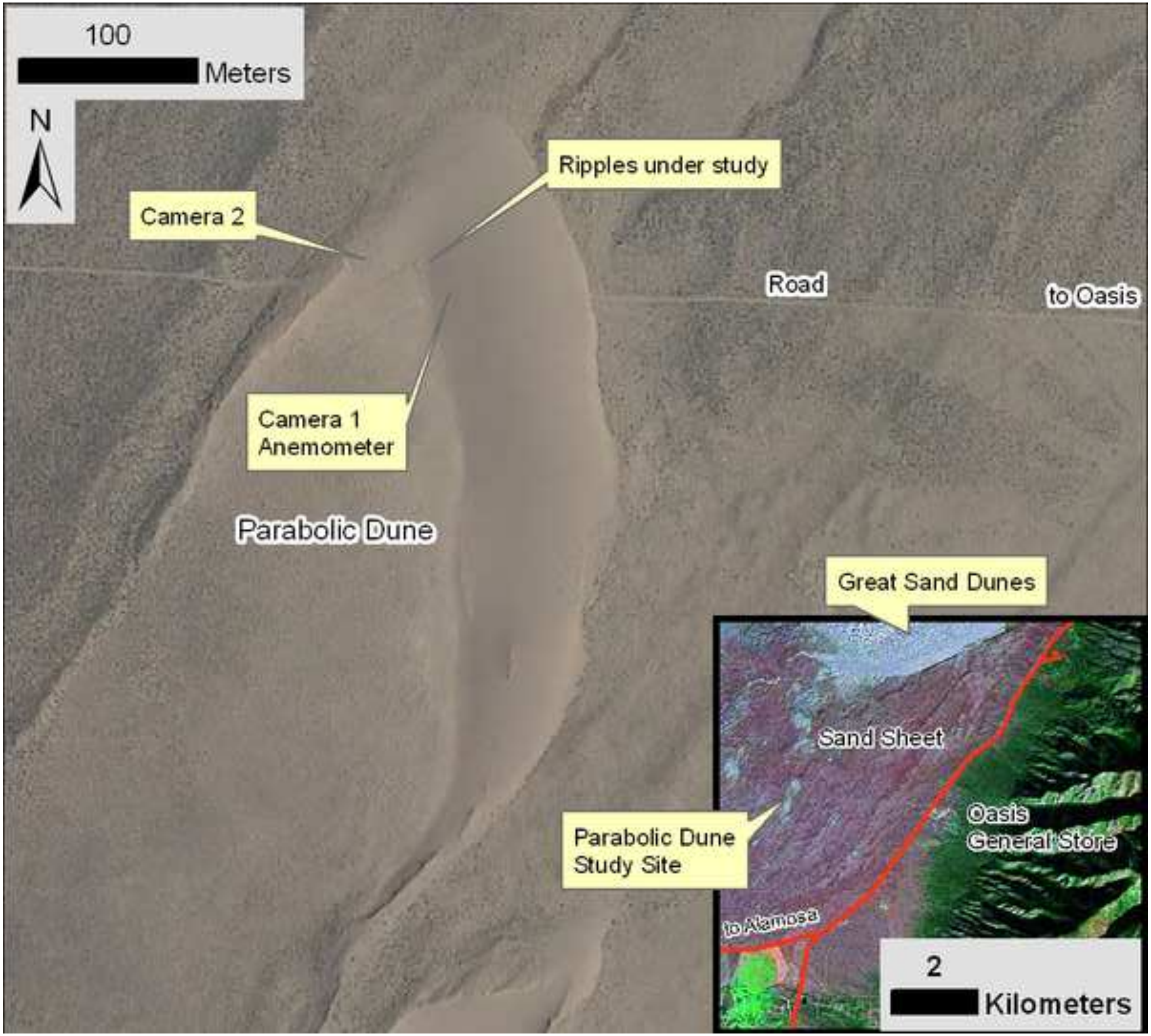

Figure 2
Click here to download high resolution image

Figure 3
Click here to download high resolution image

Figure 4
Click here to download high resolution image

Figure 5
Click here to download high resolution image

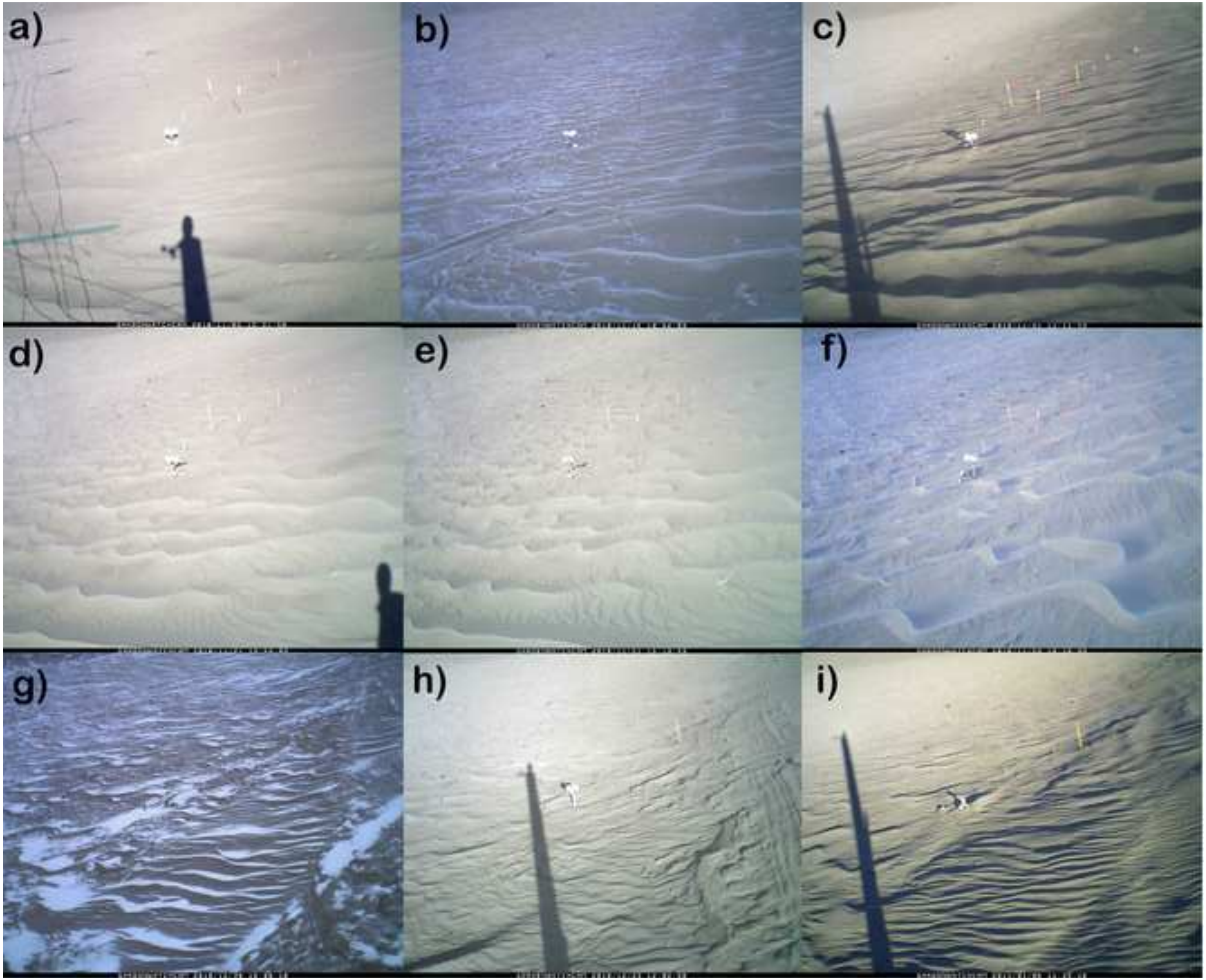

Figure 6
Click here to download high resolution image

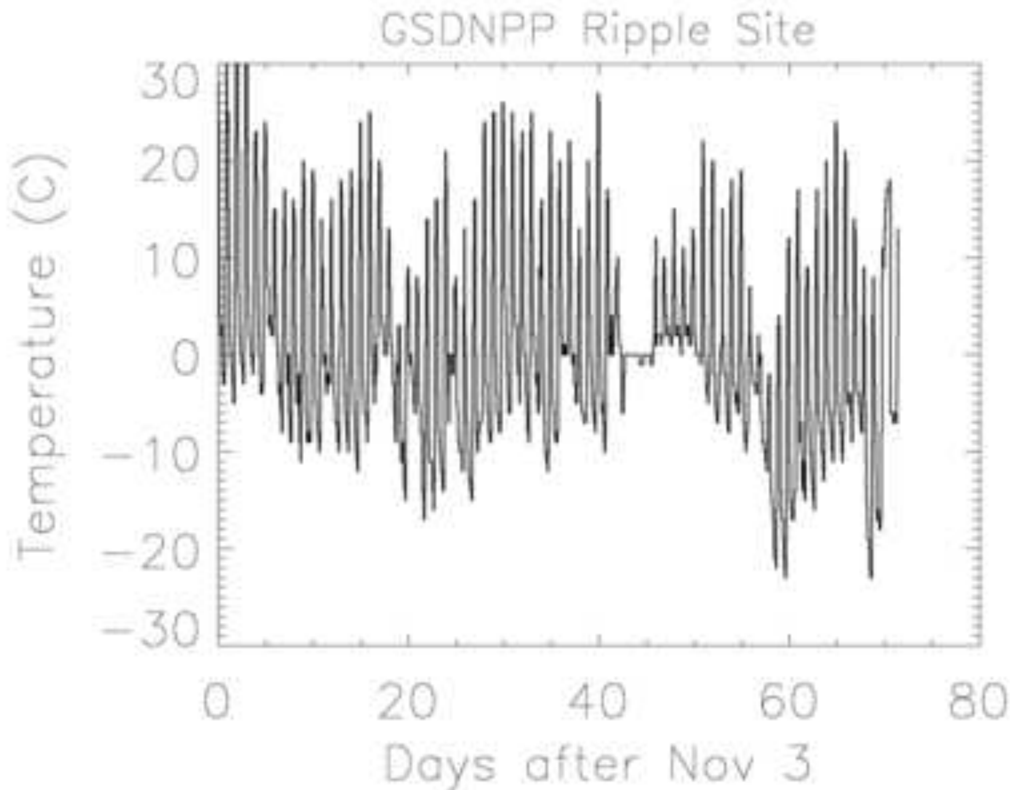

Figure 7

Click here to download high resolution image

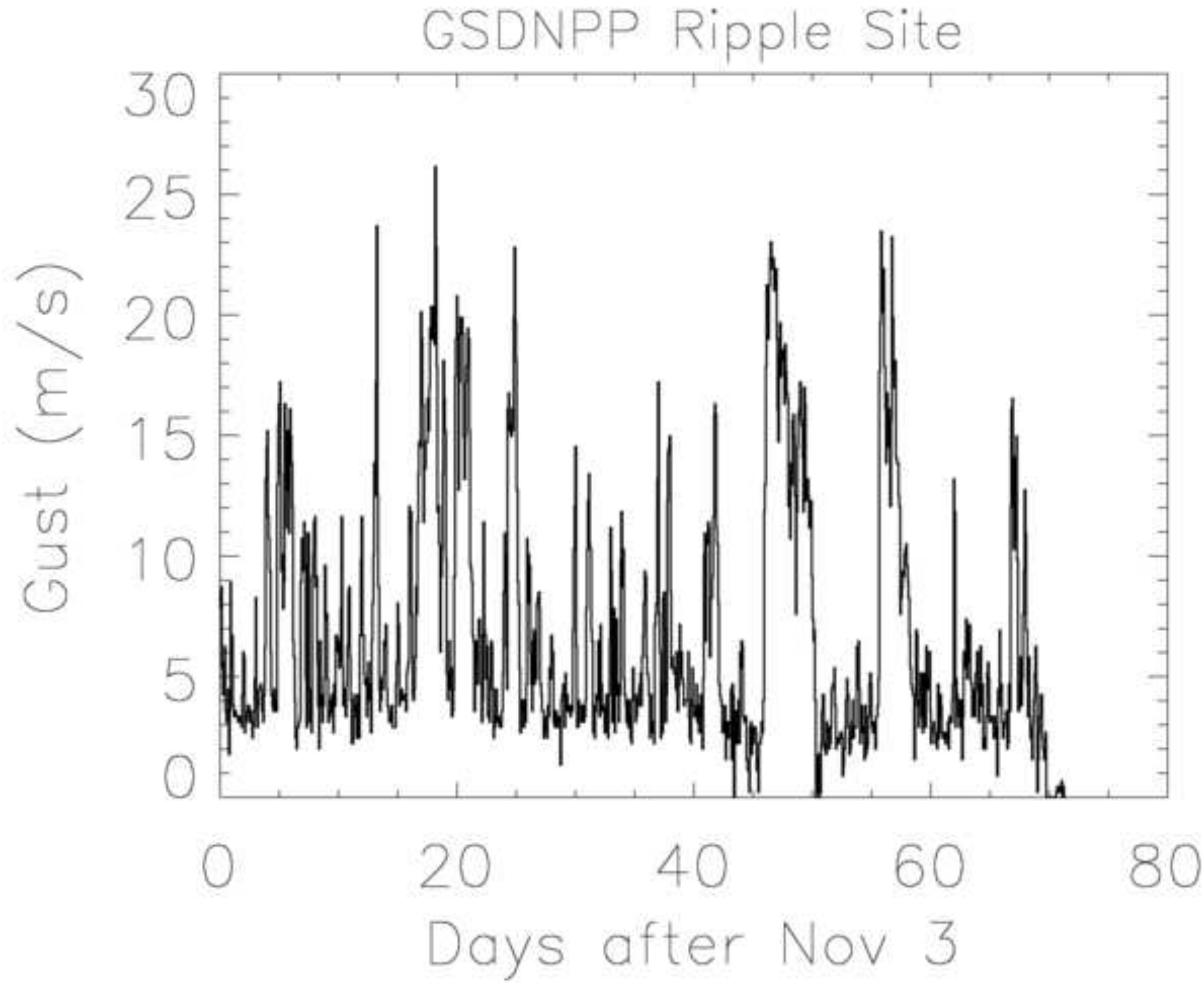

Figure 8
Click here to download high resolution image

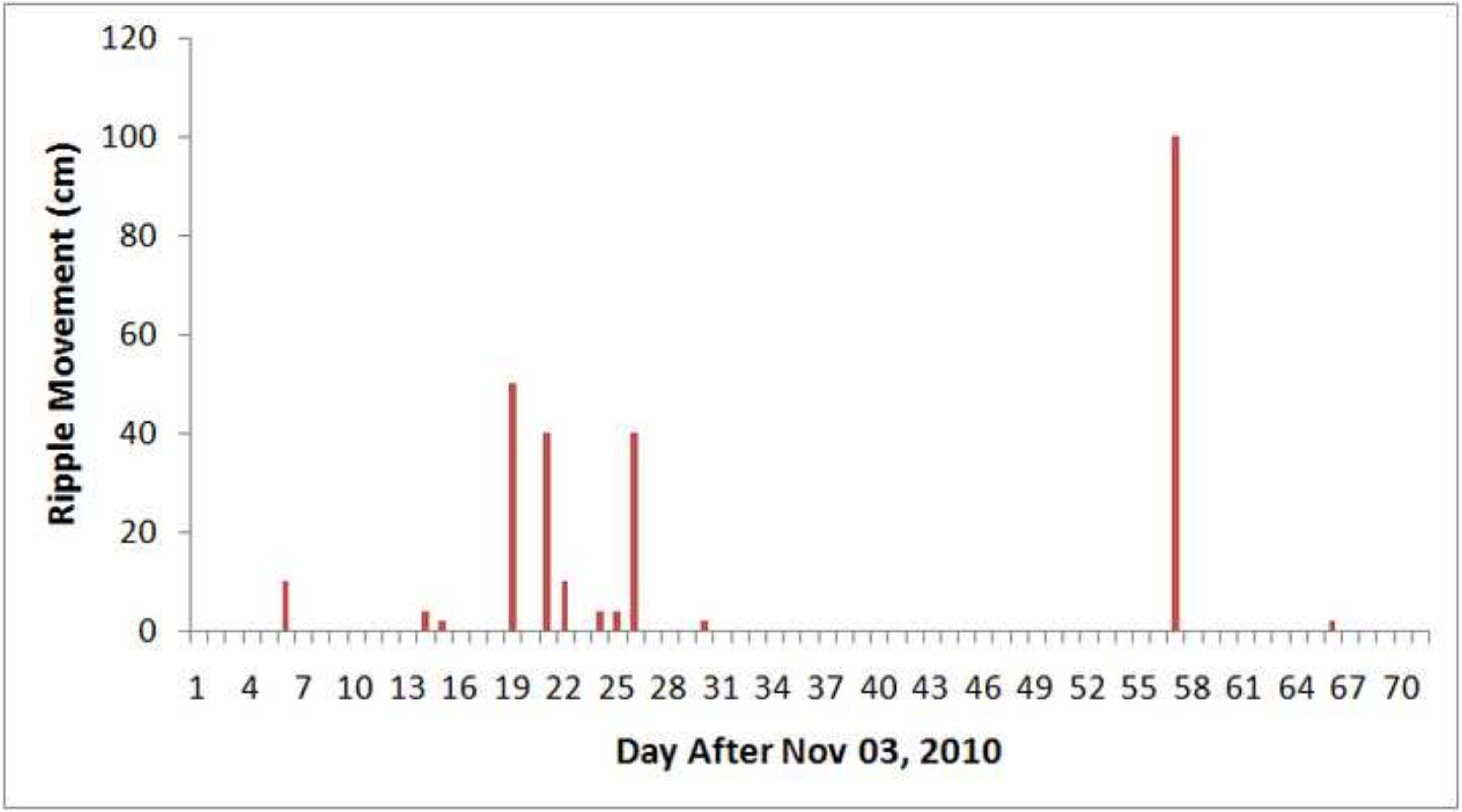

Figure 9

Click here to download high resolution image

Figure 10
Click here to download high resolution image

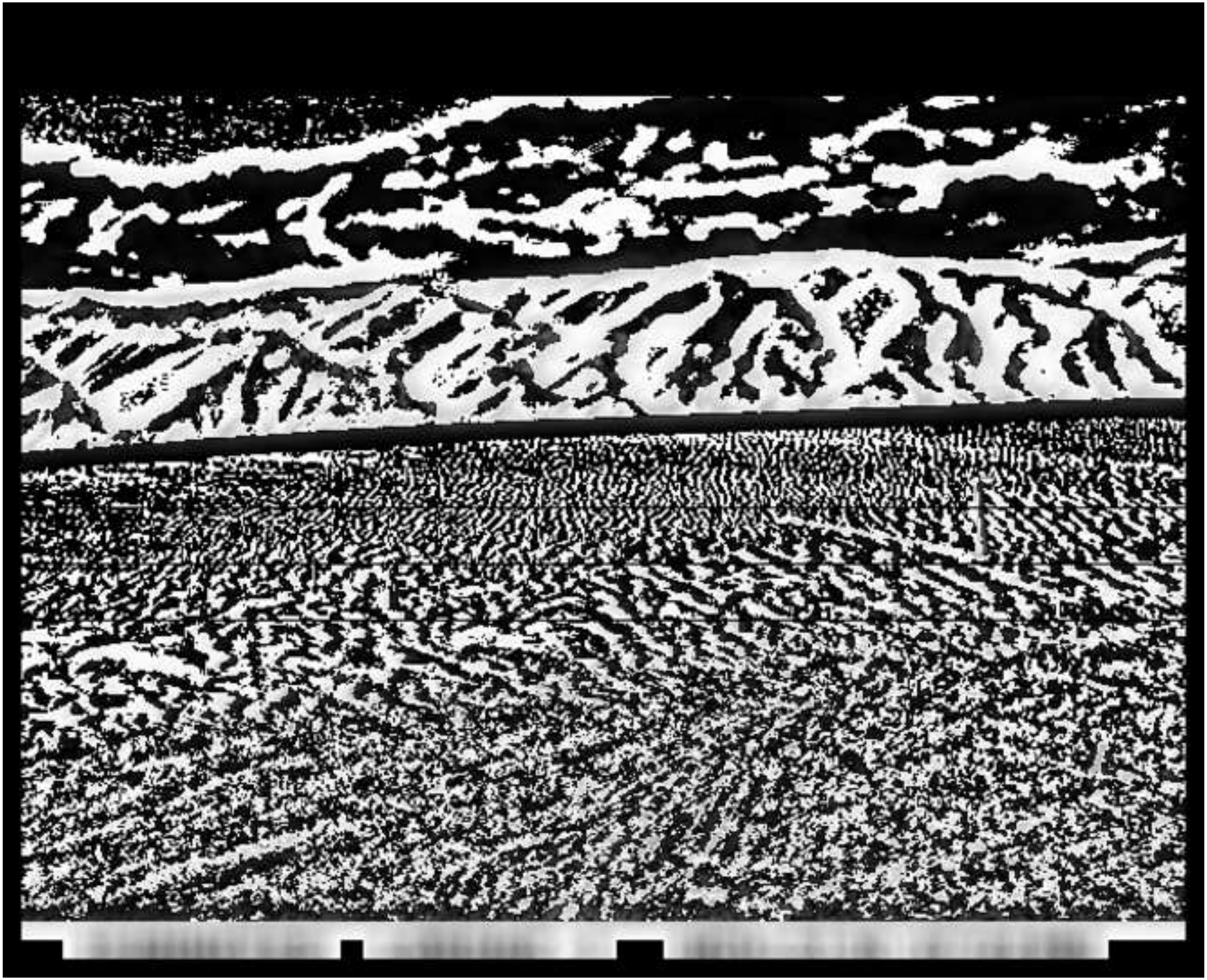

Figure 11
Click here to download high resolution image

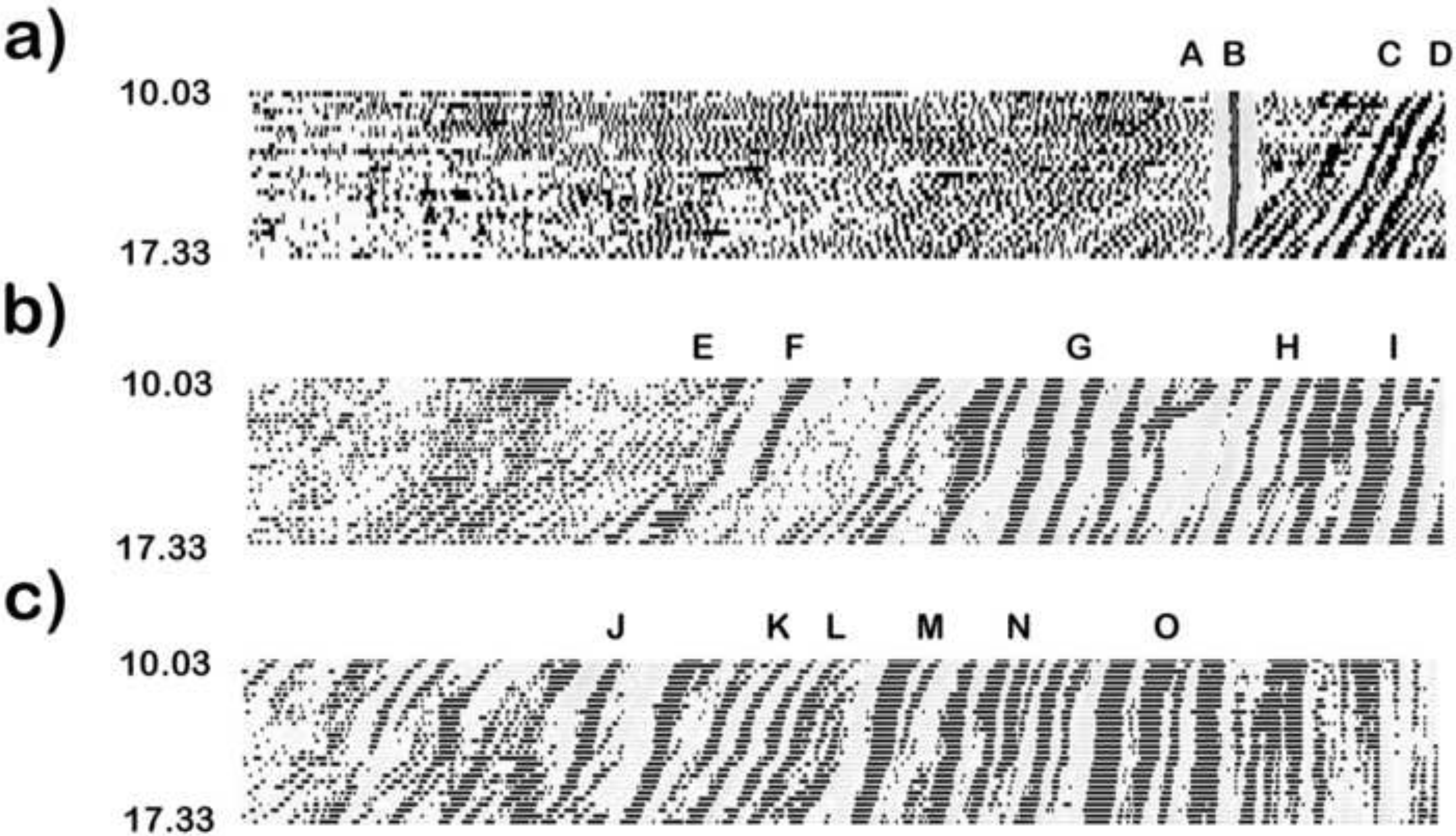

Figure 12
Click here to download high resolution image

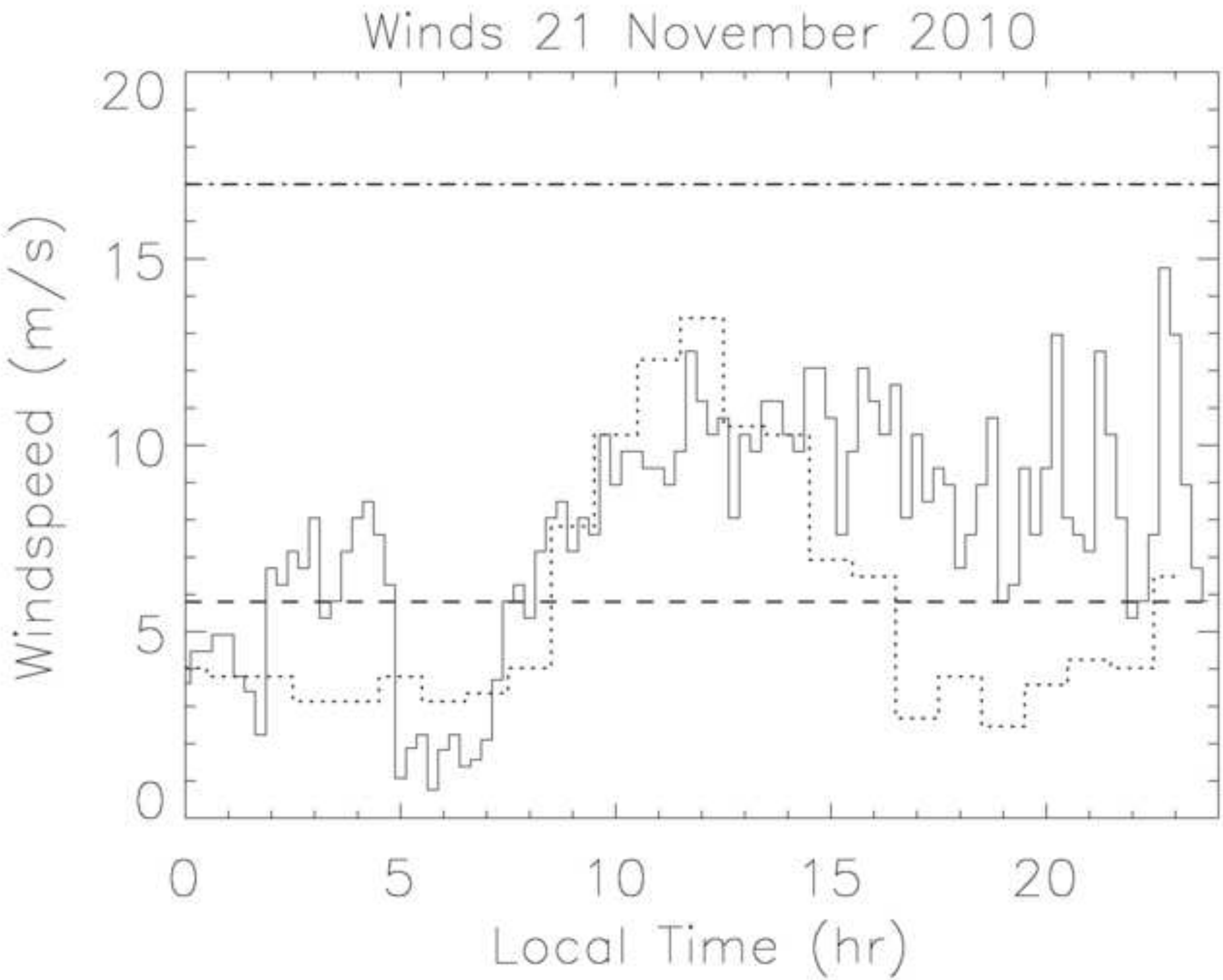

Figure 13
Click here to download high resolution image

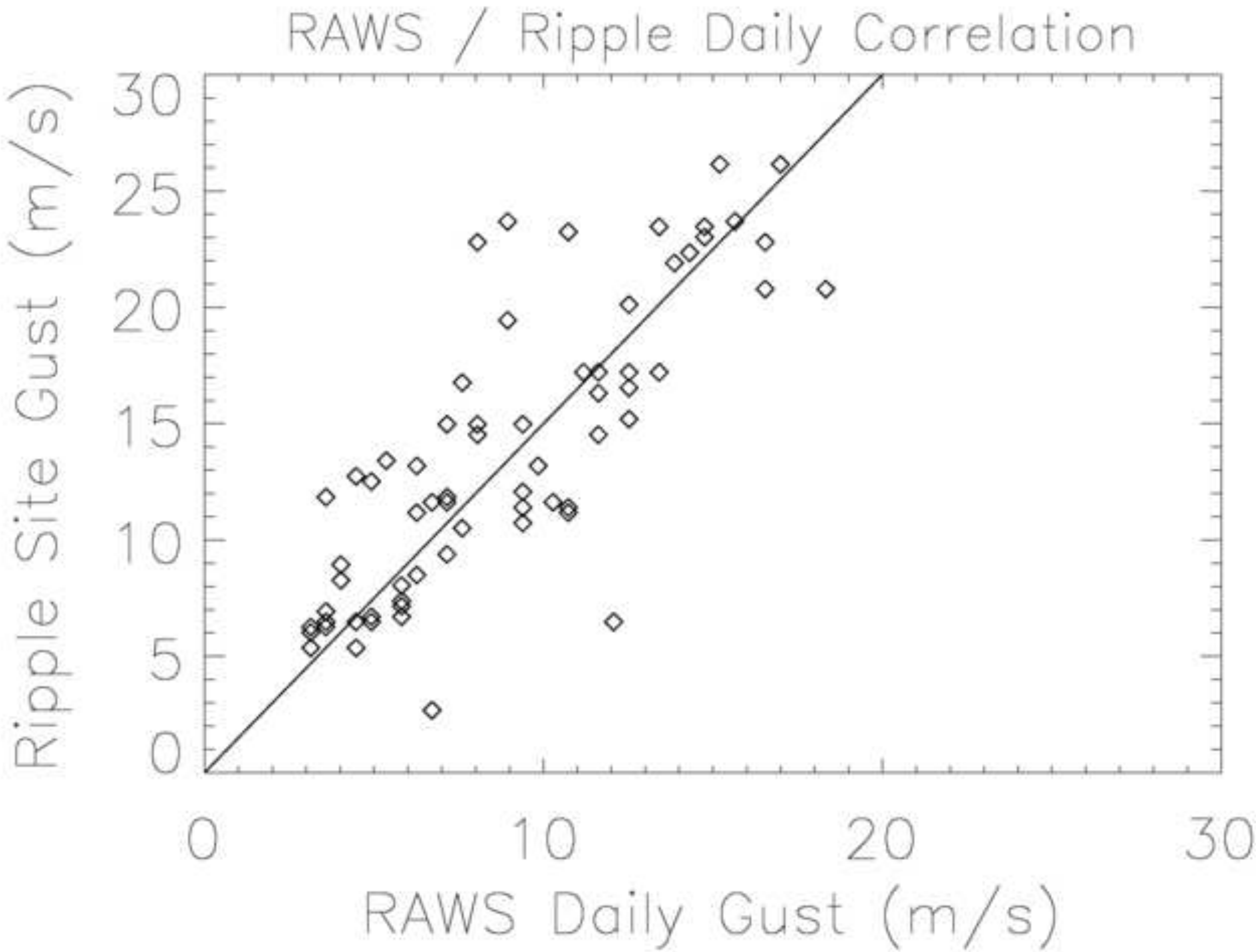

Figure 14
Click here to download high resolution image

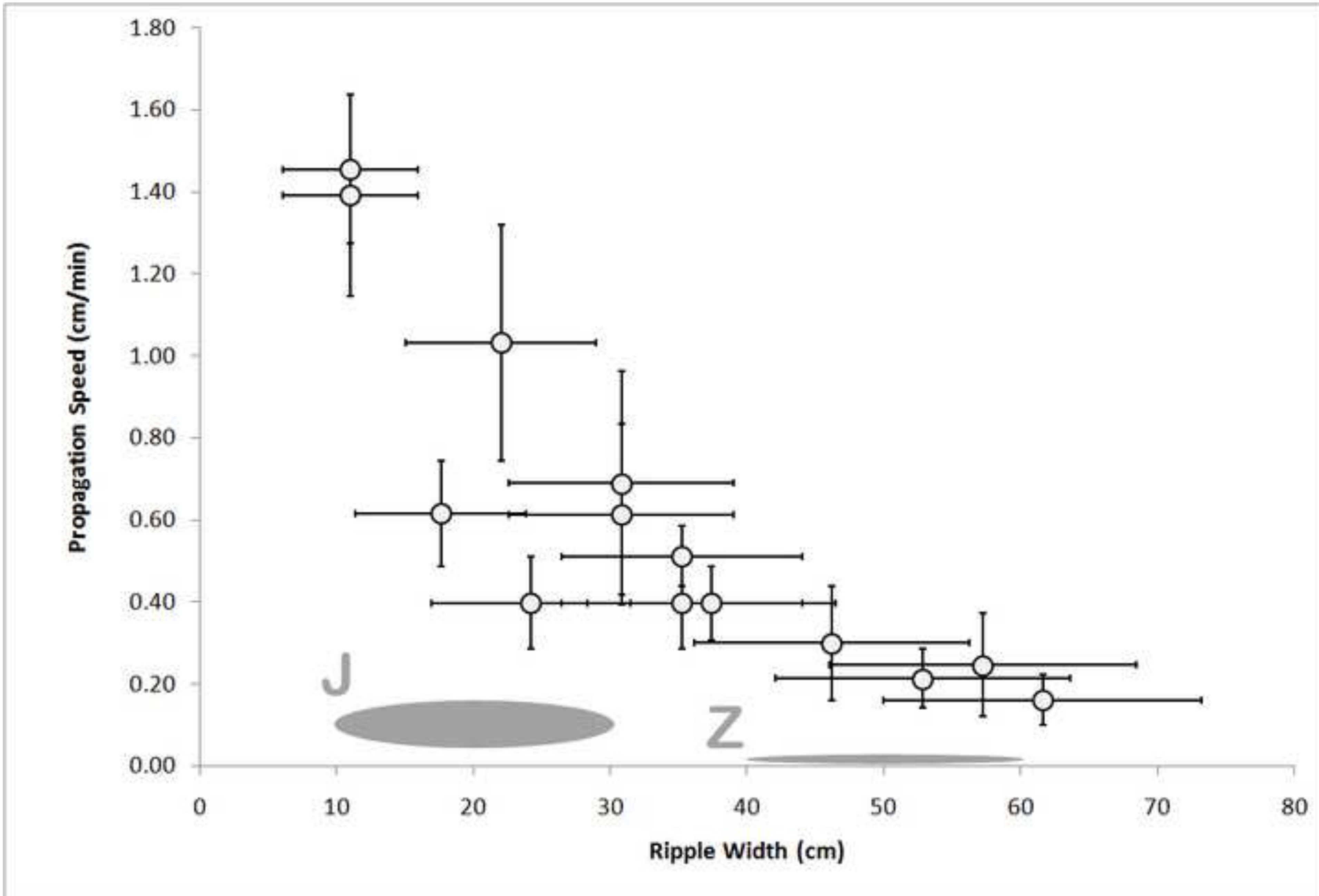

Figure 15

Click here to download high resolution image